Dynamic Biochemistry, Process Biotechnology and Molecular Biology ©2011 Global Science Books

Controlling the Curie-temperature of Magnetic Nanoparticles for Hyperthermia

Ihab Obaidat[1] • Bashar Issa[1*] • Virendra Mohite[2] • Yousef Haik[3,4]

[1] Department of Physics, United Arab Emirates University, Al-Ain 17551, United Arab Emirates
[2] Center for Nanomagnetics and Biotechnology, Florida State University, FL 32310, USA
[3] Department of Mechanical Engineering, United Arab Emirates University, Al Ain United Arab Emirates
[4] Center for Research Excellence in Nanobiosciences, University of North Carolina-Greensboro, NC, USA

Corresponding author: * **b.issa@uaeu.ac.ae**

ABSTRACT

The control of Curie temperature is very necessary in hyperthermia where cancerous cells are heated up to temperatures of 42-43°C using magnetic nanoparticles (NPs). In this paper we point out that surface spins have a major role in determining the Curie temperature of ferrite $Mn_{1-x}Zn_xFe_2O_4$ nanoparticles, where x = 0.5, 0.6, 0.8, and 1.0. The addition of Zn in $Mn_{1-x}Zn_xFe_2O_4$ is suggested to cause changes in the lattice distances. These changes are expected to be more pronounced near the surface of the NPs. Accordingly, surface disorder occurred which resulted in surface spins. Our magnetization measurements revealed several trends. For each particular x value, the field cooled (FC) magnetization of the NPs remained nearly constant at temperatures below 50 K. Above this temperature, the magnetization either exhibited peaked regions or decreased sharply. The Curie temperature also increased up to x = 0.6, and then decreased for x = 0.8 and 1.0. The existence of the initial constant magnetization and the appearance of peak regions were considered to be signatures of surface spin-glass structures. A core-shell magnetization model of the ferromagnetic surface and the ferrimagnetic core was introduced to account for these results.

Keywords: hyperthermia, Mn-Zn ferrites, nanoparticles, surface spins

INTRODUCTION

Due to finite size effects, such as the high surface-to-volume atomic ratios and different crystal structures, magnetic NPs exhibit interesting and considerably different magnetic properties than those found in their corresponding bulk materials. These new properties prompted the implementation of this type of NPs in diverse fields. But the science of magnetic NPs is still evolving in three different directions. These are; the satisfactory understanding of their physics, the synthesizing of NPs in well-specified sizes with uniform distribution, and the expanding of the fields of their applications. All these directions are currently the subject of intense research activities around the world.

Hyperthermia using magnetic NPs has been gaining a lot of interest recently as a method for curing cancer (Hergt *et al*. 1998; Berry and Curtis 2003; Mornet *et al*. 2004; Hergt *et al*. 2006; Salloum *et al*. 2008). Hyperthermia involves heating of the cancerous cells up to temperatures of 42-43°C. If heated beyond this temperature range, the normal cells are damaged which is undesirable (Deger *et al*. 2002; Park *et al*. 2002; Hergt *et al*. 2008; Thiesen *et al*. 2008). The magnetic NPs are heated when subjected to oscillating magnetic field (Berry and Curtis 2003; Mornet *et al*. 2004; Aqil *et al*. 2008; Kline *et al*. 2009). But temperatures above the 42°C (315 K) may cause necrosis (Brusentsov *et al*. 2002; Berry and Curtis 2003). A way to overcome this problem is to regulate the magnetic field and the time of exposure to this field i.e. to switch off the magnetic field as soon as the tissue temperature reaches the desired range. But since the NPs are spread around the tumor and lay at various depths inside the body, they are not uniformly heated. The NPs near the surface and closer to the source of the magnetic field have the maximum temperature whereas those located inside the body away from the source have low temperatures. Thus if the magnetic field is switched off when the surface of the NPs reach the optimum temperature range, the NPs inside the body are below this optimum temperature. Consequently the efficiency of the hyperthermia process is reduced. A solution to this problem is to use such NPs so that they stop heating up after they reach the threshold of 42°C (315 K). If the material of the magnetic NPs has a Curie temperature in the optimum heating range 42-43°C then if they are subjected to oscillating magnetic field the temperature of these will rise only up to its Curie temperature. If they are further subjected to the magnetic field of any intensity they will not be heated thereafter because beyond the Curie temperature the NPs become paramagnetic. This will also ensure a uniform heating because now the magnetic field can be kept on until all the NPs irrespective of their depth inside the body reach the optimum temperature which corresponds to their Curie temperature.

One major difficulty that underlies the use of NP therapy is the problem of getting the NPs to a particular site in the body. A potential benefit of using magnetic NPs is the use of localized magnetic field gradients to attract the particles to a chosen site, to hold them there until the therapy is complete and then to remove them. Various NPs were synthesized using physical as well as chemical methods. But since the application of NPs *in vivo* or *ex vivo* requires the NPs to be non-toxic, biocompatible and stable to the reticulo-endothelial system, the elements which are present in the human body naturally such as Fe, Ni, Mn, and Zn are preferred.

In this paper we discuss the factors that might play roles in making the ferrite $Mn_{1-x}Zn_xFe_2O_4$ NPs exhibit Curie temperature in the optimum range 42-43°C.

Received: 24 February, 2010. Accepted: 29 March, 2011.

Research Note

EXPERIMENTAL METHODS

All Mn-Zn-ferrite NPs used were obtained via chemical co-precipitation and fertilization (Patnaik 2004; Lu *et al*. 2007; Obaidat *et al*. 2009). First the m*etal* salts are co-precipitated into hydroxides. This is done by addition of aqueous solution of m*etal* salts in water to the co precipitating base (e.g. NaOH, CH_3NH_3OH, etc.). The reaction occurs as follows:

$$(1-x)Mn^{2+} + xZn^{2+} + 2Fe^{3+} + 8OH^{-}$$

$$\downarrow$$

$$(1-x)Mn(OH)_2 * xZn(OH)_2 * 2Fe(OH)_3$$

Then this precipitate is transformed into ferrite by heating in the precipitation alkaline solution (fertilization). The reaction for Mn-Zn ferrite NPs is as follows:

$$(1-x)Mn(OH)_2 * xZn(OH)_2 * 2Fe(OH)_3$$

$$\downarrow$$

$$Mn_{(1-x)}Zn_xFe_2O_4 * nH_2O + (4-n)H_2O$$

This salt solution at 90°C was added to 8M NaOH solution at 90°C followed by vigorous stirring. The stirring and heating at 90°C continued for a minimum of 40 minutes. The product was then filtered, washed with distilled water and finally washed and dried with acetone. Four samples were made, they have the form $Mn_{1-x}Zn_xFe_2O_4$ where x = 0, 0.5, 0.6, 0.8. The atomic composition was determined using X-ray powder diffraction (XRD). The magnetic measurements were conducted using Quantum Design SQUID. Field cooled (FC) magnetization measurements were conducted where a constant magnetic field of magnitude of 100 Oe was applied and the magnetic moment was measured as the temperature was varied from 0 K to 450 K.

RESULTS AND DISCUSSION

Fig. 1 shows the SEM picture for the $Mn_{1-x}Zn_xFe_2O_4$ nanoparticles, with x = 0.5. All the other SEM pictures are typical to the one shown in **Fig. 1**. As can be seen, the nanoparticles are very agglomerated due to the fact that they are not coated. The size distribution was also considerably large with an average of 30 nm.

Fig. 2 displays the magnetization hysteresis (*H-M*) curves at 5 K and 300 K for the $Mn_{1-x}Zn_xFe_2O_4$ nanoparticles, with x = 0.5. The other nanoparticles have a very similar behavior with very slight changes in the saturation and coercive fields at 5 K. We can see from figure 2 that at 300 K, the magnetization saturates soon at small magnetic field of value less than 1000 Oe. At 5 K, the magnetization does not saturate at the highest applied magnetic field value of 15,000 Oe. This non saturation of M at 5 K is attributed to large particle-particle magnetic interaction which is expected to occur for such agglomerated and non-coated particles.

Fig. 3 displays the temperature dependence of magnetization (*M-T*) for the $ZnFe_2O_4$ NPs. We can see a peculiar behavior of *M-T*. The magnetization, *M* remains nearly constant at M_o as the temperature was increased from 0 K to nearly 50 K. As the temperature was increased further, we see a sudden and large increase in *M* that occurs at a particular temperature called the spin-glass temperature, T_g. It is clearly seen that $M(T)$ forms a peaked region above T_g.

Fig. 4 shows that for x = 0.5, a similar behavior to the one presented in Figure 1 occurs. But for x = 0.6 and 0.8 the magnetization decreases sharply T = 90 K and 50 K, respectively. We believe that the peculiar $M(T)$ results (for all x values) which are displayed in these two figures cannot be explained only using the magnetic changes that occur inside the bulk of these ferrite NPs. Due to finite size effects, these results are believed to be mainly due to factors related to the surface rather than the core of the NPs. We believe that the occurrence of a significant and sudden increase of magnetization at a particular temperature is a signature of a simultaneous rotation of many surface spins along the direction of the applied magnetic field (Obaidat *et al*. 2009). This means that many spins are locked together in a group with internal pinning forces such that they will be depinned toge-

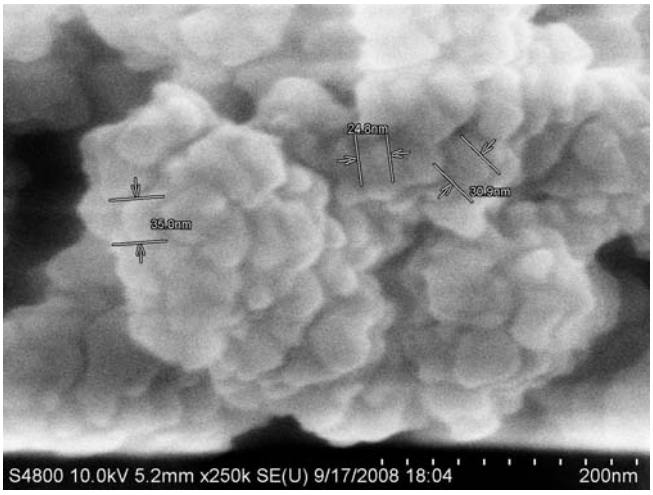

Fig. 1 SEM image of $Mn_{1-x}Zn_xFe_2O_4$ nanoparticles. x = 0.5.

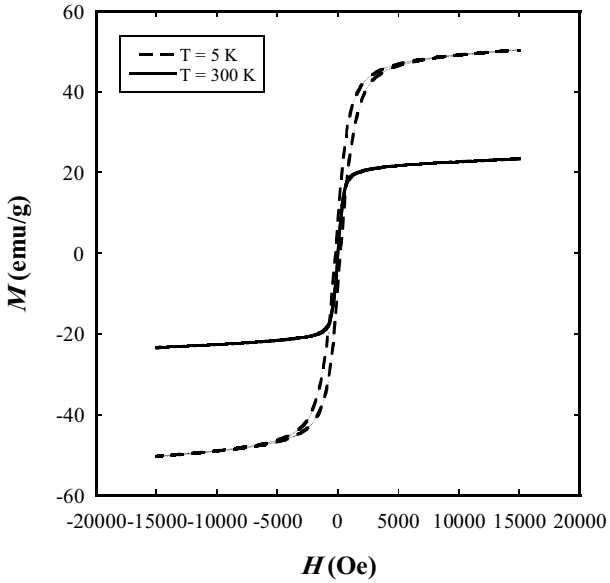

Fig. 2 Magnetization hysteresis loops for $Mn_{1-x}Zn_xFe_2O_4$ nanoparticles. x = 0.5 at 5 K and 300 K.

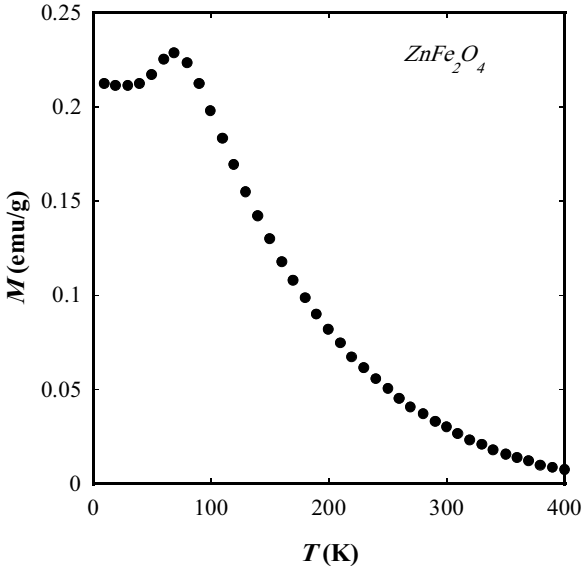

Fig. 3 Temperature dependence of magnetization, M(T), for $ZnFe_2O_4$ nanoparticles.

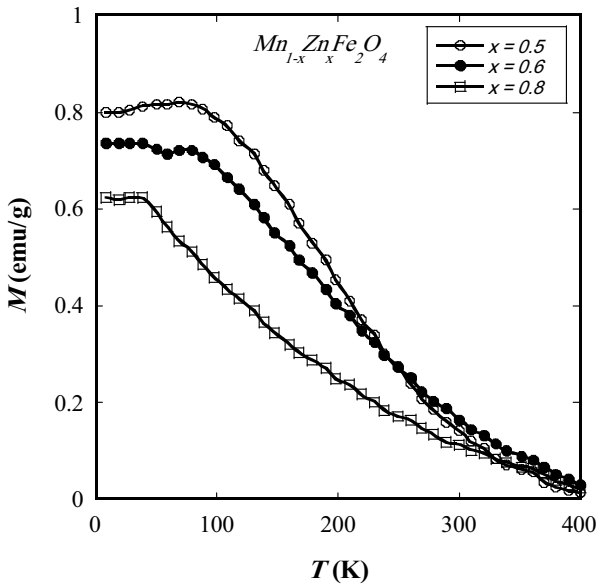

Fig. 4 Temperature dependence of magnetization, M(T), for $Mn_{1-x}Zn_xFe_2O_4$ nanoparticles. x = 0.5, 0.6, and 0.8.

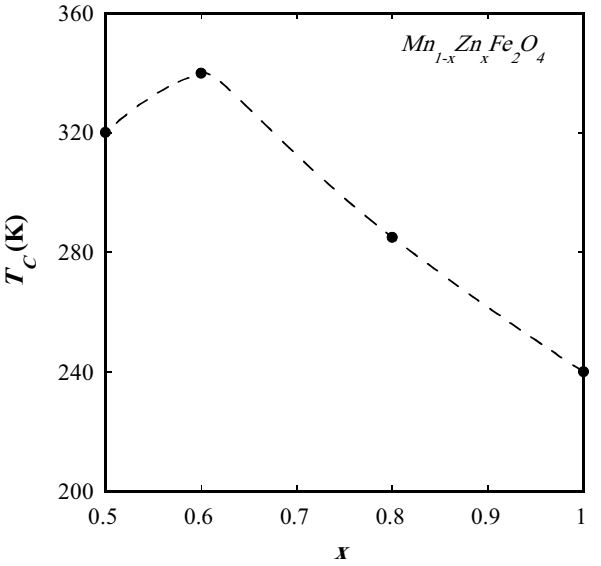

Fig. 5 Curie temperature, T_C, as a function of the Zn concentration, x for all the $Mn_{1-x}Zn_xFe_2O_4$ nanoparticles.

ther when a particular temperature is reached that cancels the internal pinning strengths. Thus we believe that the significant and sudden increase of magnetization is a signature of spin-glass phase at the surface of the NPs. The atomic disorder at the surface creates surface spins (Del Bianco *et al*. 1998; Kodama *et al*. 2006). Some of these spins are loosely pinned while some others form spin-glass structures (Kodama *et al*. 1997; Kodama and Berkowitz 1999). These spin-glass structures experience internal exchange-coupling and external exchange-bias interaction at the interface (Nogués *et al*. 2005a). The initial constant values of M for temperatures below 50 K are attributed to surface spins that are strongly pinned at the surface (Kodama and Berkowitz 1999). This behavior of M provides an evidence that the anomalous behavior of $M(T)$ is not due to the core effects because Zn does not contribute to the magnetic moment due its filled 3d and 4s shells. This behavior could be explained using a core-shell model of magnetization of NPs combined with the existence of spin-glass structures with different orientations on the surface of the NPs. In this model, the core of the NPs posses the bulk magnetization of the material, where as the shell surrounding that core posses a different kind of magnetization depending on several factors. The total magnetization of the NPs is the sum of the contributions of the core and the shell. Thus due to the small size of the NPs, the contribution of the surface magnetization is significant and can result in total magnetization which is different than that of the bulk material.

Fig. 5 displays the Curie temperature, T_C as function of the Zn concentration, x for these $Mn_{1-x}Zn_xFe_2O_4$ ferrite NPs. The Curie temperatures were calculated by extrapolation of the linear sections of the $M(T)$ curves. We can see that T_C increases with the initial increase of x and then decreases for concentration between x = 0.6 and x = 1.0. This increase and decrease of T_C is believed to be due to the increase of surface disorder as the Zn concentration is changed. The increased surface disorder resulted in more surface spins which become more resistant to thermal energy due to the increased exchange-bias interaction between the ferromagnetic surface and the ferrimagnetic core. The exchange-bias interaction changes as volume of the ferrimagnetic core changes (Shannon 1976; Nogués *et al*. 2005b; Makhlouf *et al*. 2008).

Since heating of the magnetic nanoparticles can be achieved by the magnetization hysterisis losses, it would be favorable for the hysterisis loop to be irreversible near the Curie temperature. We believe that by controlling surface morphology, the internal exchange-coupling of the spin-glass structures and the exchange-bias between the surface spins and the ferromagnetic core can be made to be significant at high temperatures, where an opening in the hysterisis loop would occur. Thus, using the core-shell model of magnetization of NPs and the existence of spin-glass structures with different orientations on the surface of the NPs, we were able to account for the behavior of the magnetization of these nanoparticles. Our model accounts for the observed constant magnetization below 50 K and the peaked-regions of magnetization above 50 K. The width of the peaked regions is suggested to depend on the internal pinning forces of the spin-glass structures and on the exchange-bias interaction between the ferromagnetic surface and the ferrimagnetic core of the NPs.

ACKNOWLEDGEMENTS

This work was financially supported by the Emirates Foundation under the Grant no. EF 29-2009/131 and by the Research Affairs at the UAE University under a contract no. 06-02-2-11/09.

REFERENCES

Aqil A, Vasseur S, Duguet E, Passirani C, Benoît J, Jérôme R, Jérôme C (2008) Magnetic nanoparticles coated by temperature responsive copolymers for hyperthermia. *Journal of Materials Chem*istry **18**, 3352-3360

Berry CC, Curtis ASG (2003) Functionalisation of magnetic nanoparticles applications in biomedicine. *Journal of Physics D: Applied Physics* **36**, R198-R206

Brusentsov N, Nikitin L, Brusentsova T, Kuzentsov A, Bayburtsky F, Schumakov L, Jurchenko N (2002) Magnetic fluid hyperthermia of the mouse experimental tumor. *Journal of Magnetism and Magnetic Material* **252**, 378-380

Deger S, Boehmer D, Turk I, Roigas J, Budach V, Loening S (2002) Thermoradiotherapy with interstitial thermoseeds in treatment of local prostatic carcinoma. Initial results of a phase II study. *European Urology* **42**, 147-153

del Bianco L, Hernando A, Multigner M, Prados C, Sánchez-López JC, Fernández A, Conde CF, Conde A (1998) Evidence of spin disorder at the surface–core interface of oxygen passivated Fe nanoparticles. *Journal of Applied Physics* **84**, 2189-2192

Hergt R, Andra W, D'Ambly CG, Hilger I, Kaiser WA, Ritcher U, Schmidt H (1998) Physical limits of hyperthermia using magnetite fine particles. *IEEE Transactions on Magnetism* **34**, 3745-3754

Hergt R, Dutz S, Muller R, Zeisberger M (2006) Magnetic particle hyperthermia: Nanoparticle magnetism and materials development for cancer therapy. *Journal of Physics: Condensed Matter* **18**, S2919-S2934

Hergt R, Dutz S, Röder M (2008) Effects of size distribution on hysteresis losses of magnetic nanoparticles for hyperthermia. *Journal of Physics: Condensed Matter* **20**, 385214.1-385214.12

Kline T L, Xu Y, Jing Y, Wang J (2009) Biocompatible high-moment FeCo-Au magnetic nanoparticles for magnetic hyperthermia treatment optimization. *Journal of Magnetism and Magnetic Materials* **321**, 1525-1528

Kodama RH, Berkowitz AE, McNiff Jr. EJ, Foner S (2006) Surface spin disorder in $NiFe_2O_4$ nanoparticles. *Physics Review Letters* **77**, 394-397

Kodama RH, Berkowitz AE, McNiff Jr. EJ, Foner S (1997) Surface spin disorder in ferrite nanoparticles. *Journal of Applied Physics* **81**, 5552-5557

Kodama RH, Berkowitz AE (1999) Atomic-scale magnetic modeling of oxide nanoparticles. *Physics Review B* **59**, 6321-6336

Lu AH, Salabas EL, Schüth F (2007) Magnetic nanoparticles: Synthesis, protection, functionalization and application. *Angewandte Chemie International Edition* **46**, 1222-1244

Makhlouf SA, Al-Attar H, Kodama RH (2008) Particle size and temperature dependence of exchange bias in NiO nanoparticles. *Solid State Communications* **145**, 1-4

Mornet S, Vasseur S, Grasset F, Duguet E (2004) Magnetic nanoparticles design for medical diagnosis and therapy. *Journal of Materials Chemistry* **14**, 2161-2175

Nogués J, Sort J, Langlais V, Doppiu S, Dieny B, Muñoz JS, Suriñach S, Baró MD, Stoyanov S, Zhang Y (2005a) Exchange bias in ferromagnetic nanoparticles embedded in an antiferromagnetic matrix. *International Journal of Nanotechnology* **2**, 23-42

Nogués J, Sort J, Langlais V, Skumryev V, Suriñach S, Muñoz JS, Baró MD (2005b) Exchange bias in nanostructures. *Physics Reports* **422**, 65-117

Obaidat IM, Haik Y, Mohite V, Issa B, Tit N (2009) Peculiar magnetic properties of MnZnGdFeO nanoparticles. *Advanced Scientific Letters* **2**, 60-64

Park BH, Koo BS, Kim YK, Kim MK (2002) The induction of hyperthermia in rabbit liver by means of duplex stainless steel thermoseeds. *Korean Journal of Radiology* **3**, 98-104

Patnaik P (2004) *Dean's Analytical Chemistry Handbook* (2nd Edn), McGraw-Hill, 1280 pp

Salloum M, Ma RH, Weeks D, Zhu L (2008) Controlling nanoparticle delivery in magnetic nanoparticle hyperthermia for cancer treatment: Experimental study in agarose gel. *International Journal of Hyperthermia* **4**, 337-345

Shannon RD (1976) Revised effective ionic radii and systematic studies of interatomic distances in halides and chaleogenides. *Acta Crystallographica* **A32**, 751-767

ThiesenB, Jordan A (2008) Clinical applications of magnetic nanoparticles for hyperthermia. *International Journal of Hyperthermia* **24**, 467-474